EJN fens EUROPEAN JOURNAL OF NEUROSCIENCE

European Journal of Neuroscience, pp. 1–9, 2011 doi:10.1111/j.1460-9568.2011.07647.x

Alpha band oscillations correlate with illusory self-location induced by virtual reality

Bigna Lenggenhager,[1,*] Pär Halje[1,*] and Olaf Blanke[1,2]
[1]Laboratory of Cognitive Neuroscience, Federal Institute of Technology, Lausanne, Switzerland
[2]Department of Neurology, University Hospital, Geneva, Switzerland

Keywords: frequency analysis, medial prefrontal cortex, multisensory integration, mu-rhythm, peripersonal space

Abstract

Neuroscience of the self has focused on high-level mechanisms related to language, memory or imagery of the self. However, recent evidence suggests that low-level mechanisms such as multisensory and sensorimotor integration may play a fundamental role in self-related processing. Here we used virtual reality technology and visuo-tactile conflict to study such low-level mechanisms and manipulate where participants experienced their self to be localized (self-location). Frequency analysis and electrical neuroimaging of co-recorded high-resolution electroencephalography revealed body-specific alpha band power modulations in bilateral sensorimotor cortices. Furthermore, alpha power in the medial prefrontal cortex (mPFC) was correlated with the degree of experimentally manipulated self-location. We argue that these alpha oscillations in sensorimotor cortex and mPFC reflect self-location as manipulated through multisensory conflict.

Introduction

Neuroscientific and philosophical theories stress the importance of bodily processes in self-consciousness (Berlucchi & Aglioti, 1997; Gallagher, 2005; Metzinger, 2007). Experimentation with bodily stimuli is complex as bodily inputs are continuously present and are characterized by information from the motor system as well as many different senses, including tactile, proprioceptive, nociceptive and vestibular (for a review, see e.g. Lackner & DiZio, 2000). Recent behavioural work (Ehrsson, 2007; Lenggenhager *et al.*, 2007; Petkova & Ehrsson, 2008; Aspell *et al.*, 2009; Lenggenhager *et al.*, 2009) has developed experimental techniques to manipulate and study bodily self-consciousness by providing ambiguous multisensory information about the location and appearance of one's own body using video-based technology. Following one line of such research, synchronous stroking of the participants back with a seen body in front of them (Lenggenhager *et al.*, 2007) led to changes in global aspects of self-consciousness, such as self-location or self-identification with a body (Blanke & Metzinger, 2009). What brain mechanisms are underlying these changes? Studies in patients with abnormal bodily self-consciousness pointed to a disturbance of multisensory processes, in particular in the temporo-parietal cortex (Blanke *et al.*, 2002, 2004; De Ridder *et al.*, 2007), but also in the frontal and parietal cortices (Heydrich *et al.*, 2011; Lopez *et al.*, 2010).

Correspondence: Dr B. Lenggenhager, Social and Cognitive Neuroscience Laboratory, Psychology Department of 'Sapienza', Via dei Marsi 78, 00185 Rome, Italy.
E-mail: bigna.lenggenhager@gmail.com

*B.L. and P.H. contributed equally to this study.

Received 4 November 2010, revised 12 January 2011, accepted 7 February 2011

Here we further developed our previous research protocol to manipulate self-location (Lenggenhager *et al.*, 2007) by using virtual reality (VR) technology, optical tracking, real-time projection (on a large-size screen) and the measurement of the associated brain activity [high-resolution electroencephalography (EEG)]. We analysed changes in the alpha (8–13 Hz) and gamma (30–50 Hz and 30–100 Hz) bands because of their association with multisensory integration and self-related processing. Alpha band power over the sensorimotor cortex has been linked to the perception of human bodies and the mirror neuron system, and is an index of motor (Pineda, 2005) and somatosensory (Pfurtscheller, 1981) activities. It has for example been linked to the degree of identification with the observed actor or action (Oberman *et al.*, 2005), and to human touch viewed from egocentric vs allocentric perspectives (Cheyne *et al.*, 2003). Accordingly, we predicted that alpha band power over (pre-)motor and/or somatosensory areas would also reflect changes in bodily self-consciousness (self-identification and self-location). This is in line with previous findings that linked the related rubber hand illusion to premotor and parietal cortices (Ehrsson *et al.*, 2004). We thus expected to find body-specific alpha/mu band suppression depending on the synchrony of stroking.

Gamma oscillations have previously been linked to integration across different sensory modalities into a coherent percept (Senkowski *et al.*, 2007). Neuronal systems involved in these processes are likely to be engaged during the manipulation of self-location through visuo-tactile conflict. In accordance with this idea, an increased power in the lower gamma band (30–50 Hz) over parietal scalp regions was found during the integration of tactile and visual cues in peripersonal space in a rubber hand illusion-like paradigm (Kanayama *et al.*, 2007, 2009). We therefore hypothesized body-specific

increases in gamma power during synchronous as compared with asynchronous stroking.

Materials and methods

Participants

Eleven healthy, right-handed volunteers (three women, mean age: 21 ± 1.7 years, SD) participated. One participant was excluded from the analysis of the drift because of missing data in one condition. All participants had normal or corrected-to-normal vision, and written informed consent was obtained prior to their inclusion in the study. The study protocol was approved by the local ethics research committee of the University of Lausanne, and has been performed according to the ethical standards as declared in the Declaration of Helsinki.

Experimental procedures

Participants stood 2 m in front of a large rear-projection screen (3.2 m wide, 2.35 m high) displaying a life-sized, back-facing virtual body or a cubic control object. We manipulated self-location through the synchronous or asynchronous stroking of both the back of the virtual character as well as the virtual object (Fig. 1).

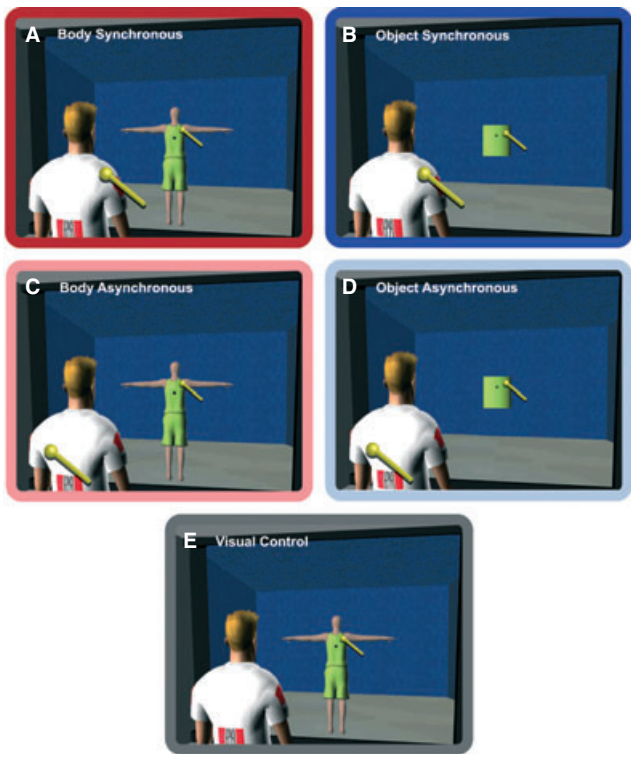

FIG. 1. Experimental conditions. Participants (shown in white EPFL t-shirt) were stroked on their back with a motion-tracked stick (stick at the back of the participant) whose motion was projected synchronously (A and B) or asynchronously (C and D) to the virtual stick (stick depicted on the large screen; border of the projection screen is indicated in black). The projection screen was 2 m in front of the participant. The virtual stick was stroking either a virtual body (A and C) or a cube-like control object (B and D). As a control condition (E), we added a condition where the participant was observing stroking on the virtual body (as in A and C), but during which no stroking was applied to the participant's back. The colour of the frame for each plot (red, A; pink, C; dark blue, B; light blue, D) depicts the colour code for each condition used in all other figures.

Participants wore an EEG cap and a belt with two optical markers to track and measure their body sway. The motion tracking data were used to animate the virtual character on the screen in real-time. White noise was delivered through headphones to mask any auditory cue about body location and stroking pattern. To prevent participants from seeing anything but the screen, they wore a shield limiting the visual angle to approximately 95 °. After familiarization with the stimuli and the experimental protocol, participants were asked to stand as still as possible and fixate a small dot in the centre of the screen (coinciding with the centre of the virtual object).

Four experimental conditions were used (Fig. 1A–D). Participants were stroked on their back with a motion-tracked stick, and the virtual stick moved either synchronously with the real stick (real-time motion capture; Fig. 1A and B) or asynchronously (replay of a previously recorded stroking period; Fig. 1C and D) on either a virtual human body (animated, gender-specific character; Fig. 1A and C) or a control object (cube; Fig. 1B and D). Additionally, we measured one control condition where the participants were not touched but still saw pre-recorded stroking on the virtual body (visual condition; Fig. 1E). We included this visual baseline condition in the paradigm because of our concern that the asynchronous conditions contained a cross-modal conflict that the synchronous conditions lacked; thus, it would not have been possible to separate any activation related to a change in self-location from purely conflict-related activations (e.g. Keysers *et al.*, 2004). The same recording of the moving stick was used to animate the asynchronous condition and the visual condition. In all conditions the participant's body sway was projected in real-time to the virtual object. The five conditions were presented in random order. Each condition lasted 4 min, and participants were instructed to continuously indicate by button press (Wiimote device; Nintendo, Kyoto, Japan) if the touch they saw and the touch they felt were the same or not. The exact instruction was: 'Please press the A-button whenever the touch you see and the touch you feel are the same/congruent and the B-button when they are not'. This was a forced choice judgement and participants were always pressing one of two buttons. The results of this task show that participants perceived the stroking to be the same 88% (± 3 SD) of the time in the synchronous body condition and 83% (± 12 SD) of the time in the synchronous control object condition. The corresponding values for asynchronous stroking were 16% (± 11 SD, asynchronous body condition) and 15% (± 11 SD asynchronous control object condition). The body and control object conditions did not significantly differ ($P \geq 0.05$, dependent *t*-test).

Immediately after each 4-min stroking period, the screen turned black and participants were passively moved back by approximately 1.5 m while their eyes were closed. They were then asked to return to where they thought they were located during the stroking (Lenggenhager *et al.*, 2007). The moving trajectory (including the final relocation error, i.e. drift in self-location) was recorded with the tracking system.

Motion capture and visual feedback

An active optical motion capture system (ReActor 2; Ascension Technology, Burlington, VT, USA) was used for tracking and recording of movements with a capture rate of 30 Hz. Two active, optical infrared markers were used to track the participant's body (one was positioned in the front under the umbilicus, the other over the right hip). One marker was placed on the stroking stick and was used to track the stroking. Each marker contained light-emitting diodes (LEDs), and the LED signals were detected by 448 detectors embedded in a 12-bar cuboid frame of the dimensions 4.11 m (length) × 4.11 m (width) × 2.54 m (height). The area within which

body movements can be tracked is 3.0 m (length) × 3.0 m (width) × 2.4 m (height). Data transfer to a desktop computer was wireless, which allowed the participant to move around freely.

A commercial, real-time productivity suite was used for the 3D animation of the virtual room and objects (MotionBuilder Software; Autodesk, San Rafael, CA, USA). This software facilitates implementing the real-time data from the motion capture system and the mapping to virtual objects. The overall delay of the system, including data acquisition, character animation and visual projection, was < 80 ms. The visual stimuli were (back-) projected with a JVC DLA-SX21 (JVC USA, Wayne, NJ, USA) projector with high resolution (1280 × 1024 pixels). The projection screen formed one of the walls of the tracking arena. The dimensions of the virtual room, the camera position and the field of view were chosen such that the virtual scene appeared to be a natural extension of the real room from the participant's point of view. The virtual body shown on the screen appeared to have the same proportions as an actual person standing at the same distance.

EEG acquisition

Continuous EEG was acquired with a Biosemi system (Biosemi, Amsterdam, the Netherlands) from 256 pre-amplified scalp electrodes (2048 Hz sampling rate at 24 bits). The EEG was recorded in standing participants during each of the five experimental procedures. The active reference electrode pair ('CMS-DRL') was placed close to the apex. An average reference was used for all offline analysis of the data. Four additional electrodes were used to monitor artefacts related to eye movements and eye blinks. These electrodes were placed above and below the dominant eye, and horizontally near the left and right lateral canthi.

EEG data processing

Electrodes with DC offsets larger than 50 μV with respect to the CMS electrode were excluded from analysis. The average number of included channels was 208 (81%). Time periods artefacted by eye blinks and transient changes in electrode-to-scalp conductance were identified by an automated algorithm. Eye blinks were detected by taking the difference between the upper and lower eye channel, low-passing that signal at 5 Hz, calculating the numerical derivative $V'(t) = (V(t + 1) - V(t))/\text{SamplingFreq}$, and finally defining time-frames as artefacted if the absolute value of V' was larger than a fixed threshold. The threshold was set individually for each subject and ranged from 700 to 1200 μV/s. Transient changes in conductance were detected by first smoothing the average referenced EEG channels temporally by convoluting the signal with a sliding 0.1-s Gaussian window $w(t) = \exp(-1/2*(\alpha t)\text{^}2)$, $-1 < t < 1$, $\alpha = 2.5$. The slide step was 10 ms. The absolute value of the numerical derivative of the smoothed signal was thresholded; any timeframe with a value above a certain threshold was marked as artefacted. The threshold was set individually for each subject and ranged from 2 to 5 mV/s. In addition, all EEG data were visually inspected as in previous studies (e.g. Tadi *et al.*, 2009). For each participant and experimental condition, 2-s epochs were allocated across the 4-min block in such a way that they did not overlap with any artefacted timeframes. If multiple epochs could be fitted into an artefact-free period, those epochs overlapped each other with 1 s.

The power spectral density was calculated for each single epoch using a Fast Fourier Transform (FFT; Matlab, MathWorks, Natick, Massachusetts, USA) with 4096 points (0.5 Hz frequency resolution). To minimize edge effects, the linear trend was removed and a Hann window was applied before performing the Fourier transformation (Blackman & Tukey, 1959). On average, 160.2 ± 34.6 epochs survived per condition and per participant, and there was no significant difference in the number of included epochs compared across conditions (ANOVA, $P = 0.16$, $F = 1.76$). The power spectra were averaged for each participant, electrode and condition separately. This resulted in five power spectra per participant and per electrode (Synchronous Body, Asynchronous Body, Synchronous Object, Asynchronous Object, Visual Control; Fig. 1).

EEG statistical analysis

Band power contrasts

According to our hypothesis (see Introduction) we performed the following statistical tests for the alpha (8–13 Hz) and gamma bands (low: 30–50 Hz; broad: 30–100 Hz). Our interest in the low-gamma band stems from previous EEG studies of a rubber hand illusion-like paradigm that suggested an involvement of the 30–50-Hz range in the visual–tactile integration in the peripersonal space (Kanayama *et al.*, 2007, 2009). Two-sided *t*-tests were used to test for significant differences ($P < 0.05$) in log-band power as compared with the control condition. The logarithm of the power ratios was used in order to improve the normality of the power ratio distribution (Oberman *et al.*, 2005). Due to electrical noise, 49.5–50 Hz FFT coefficients were excluded from the gamma band averages. The tests were performed across all participants for each electrode individually, and resulted in one scalp map of significant electrodes for each experimental condition.

The significant electrodes were grouped in clusters and we performed further statistical analysis on these clusters. We defined electrode clusters formally by declaring an electrode as part of a cluster if it was a neighbour of an electrode in that cluster. We defined two electrodes as being neighbours if they were separated by < 2.5 cm (average neighbourhood size of five electrodes). No electrode was neighbourless using this definition.

We controlled for Type I errors by estimating the false discovery rate of different cluster sizes. This was achieved with a permutation test, which we adapted from standard methods used in functional magnetic resonance imaging and positron emission tomography (suprathreshold cluster test; Nichols & Holmes, 2002), as well as EEG and magnetoencephalography (Maris & Oostenveld, 2007) – a permuted data set was created by interchanging the power maps between the two compared conditions for half of the participants. Because there are 462 different ways of choosing five (nearly half) participants out of 11, we could construct 462 unique permuted data sets. A significance map was calculated for each permuted data set in the same way as for the unpermuted data (paired *t*-test, $P < 0.05$). The significant electrodes were grouped into clusters and the number of electrodes in the largest cluster was recorded for each permutation to create a reference distribution of maximum cluster sizes. Based on this distribution, we declared a cluster in the unpermuted set to be significant at the α-level if it was larger than $100 \times (1 - \alpha)$% of the clusters in the distribution. This secondary significance level was set to $\alpha = 0.05$ (but note that it is conceptually independent from the primary, *t*-test threshold, which also was 0.05).

Correlations between drift and band power

The linear correlation coefficient between log-band power (mean value of all epochs included in the 4-min condition) and drift in estimated self-location (one measurement at the end of each 4-min condition) was calculated for each electrode. For both power and drift

we used the values from the synchronous conditions relative to the asynchronous conditions (body or control object, respectively). The probability for a linear relationship was tested (*t*-statistic with 9 ° of freedom using Matlab). Clusters of significantly correlated electrodes ($P < 0.05$) were defined as above.

To correct for Type I errors we performed a permutation test similar to the one above. The original data consisted of one drift measurement and one power value per participant per channel, and each permuted data set was created by pairing the drift and the power values randomly between participants. Note that the pairing was always done in the same way for different electrodes to preserve any spatial correlations. Because there were $11! \approx 4 \times 10^7$ ways to permute the data, we selected 10 000 permutations randomly and created the distribution of maximum cluster sizes based on that selection. As above, the secondary *P*-value threshold was set to 0.05.

Source localization

The software package sLORETA (Pascual-Marqui, 2002) was used to estimate the neural generators of the EEG scalp measurements. The sLORETA method calculates electric current densities from scalp potentials by using a pseudo-inverse of the electrical lead field. The lead field was derived from the MNI152 template with a three-compartment boundary element head model (Fuchs *et al.*, 2002). We calculated the inverse transformation matrix using a signal-to-noise regularization of 1. The inverse transformation was applied to average cross-spectra (one average per subject and condition). Statistical maps were calculated either by comparing two inverse solution maps by means of two-tailed, paired *t*-tests (band power contrasts), or by performing linear regression with an external variable on several maps (drift correlation). The statistical maps were corrected for Type I errors (SnPM; Nichols & Holmes, 2002). Before statistical comparisons, all inverse maps were log transformed and subjected to participant-wise normalization (Pascual-Marqui, 2002).

Results

We first describe the behavioural results concerning self-location as measured by drift (Lenggenhager *et al.*, 2007) for the four experimental conditions (Fig. 1A–D). Next we describe the EEG results where we first report the comparison of the four experimental conditions in the alpha and gamma band power. Finally, we describe the correlations between the drift and the electrophysiological measures. Behavioural and EEG measurements in these four experimental conditions are analysed relative to a visual baseline condition (see, e.g. Oberman *et al.*, 2005; for a similar approach) during which the participants saw the stroking of the virtual body without being touched on their own back (Fig. 1E).

Behavioural measure – self-location

Compared with the visual control (baseline) condition, in the synchronous body condition we found a significant drift in self-location (in the anterior–posterior axis) that was characterized by a deviation of 17.3 cm (± 5.6 SEM) towards the virtual body ($P = 0.01$, $t = 3.1$, two-tailed *t*-test; Fig. 2). This was not the case in the synchronous control object condition where participants showed a smaller, non-significant drift of 10.1 cm (± 8.0 SEM) in the same direction ($P = 0.24$, $t = 1.3$). In both asynchronous conditions the drift was negative and thus in the direction away from the virtual body [body: −5.5 cm (± 10.3 SEM); control object: −7.4 cm (± 6.1 SEM)], and did not differ significantly from the visual control condition ($P_{body} = 0.61$, $t_{body} = 0.5$; $P_{control\ object} = 0.26$, $t_{control\ object} = 1.2$).

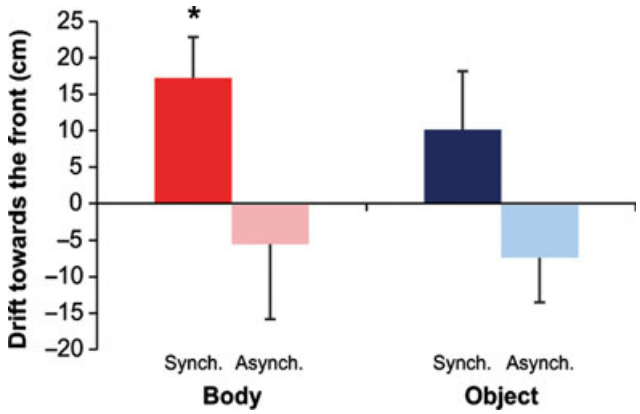

FIG. 2. Self-localization. Drift in the different experimental conditions is shown. Positive values indicate drift towards the virtual object (body or cube; mean ± SEM) as compared with the visual control condition (measured in cm). This measurement was taken after synchronous (dark colours) and asynchronous (light colours) stroking of either the virtual body or the control object. *Indicates the significant difference between the synchronous body condition and the control condition ($P < 0.05$).

None of the conditions differed significantly from the visual control condition in the orthogonal (left–right) axis. A 2 × 2 ANOVA with the factors Object (body/control object) and Synchrony (synchronous/asynchronous) showed a significant main effect of Synchrony ($P = 0.005$, $F = 13.1$). The same analysis for deviations in the left–right axis did not reveal any significant main or interaction effects.

Alpha and gamma band oscillations in the four experimental conditions

Alpha band power

We used two-sided *t*-tests (with the log of the alpha power value for each electrode) to compare the alpha power in each condition with the visual control condition. After correction (see Materials and methods; Supporting Information Figs S2 and S3) we found a large cluster of 23 electrodes ($P = 0.046$) over bilateral sensorimotor areas that was significantly different from the control condition, showing significantly less power in the alpha band in the asynchronous body condition (Fig. 3A–D). Analysing the cluster average, we found that only the asynchronous body condition differed significantly from the visual condition (two-tailed *t*-test, $P = 0.005$, $t = 3.6$; Fig. 3E). A 2 × 2 ANOVA with the values relative to the visual condition showed a main effect of synchrony ($P = 0.006$, $F = 11.9$) with stronger suppression in the asynchronous conditions. See the Supporting Information (Figs S1 and S2) for more detailed data, including power maps and uncorrected statistical maps. The inverse solution (sLORETA) localized the electrical generator of these alpha band changes in the asynchronous body condition to medial sensorimotor and premotor cortices (including the precentral gyrus and the posterior superior frontal gyrus) of both hemispheres. The maximum was localized in the left precentral gyrus ($F = 3.29$; MNI: $X = -10$, $Y = -10$, $Z = 65$; Fig. 3F). We also compared alpha band oscillations directly between synchronous and asynchronous conditions. This was done separately for body and control object conditions. The results for these comparisons show only for the body conditions an activation pattern that is highly similar to the asynchronous vs. visual-only comparison (yet with opposite sign). No differences were found in the object comparison. This confirms that the activation in the synchronous condition is not significantly

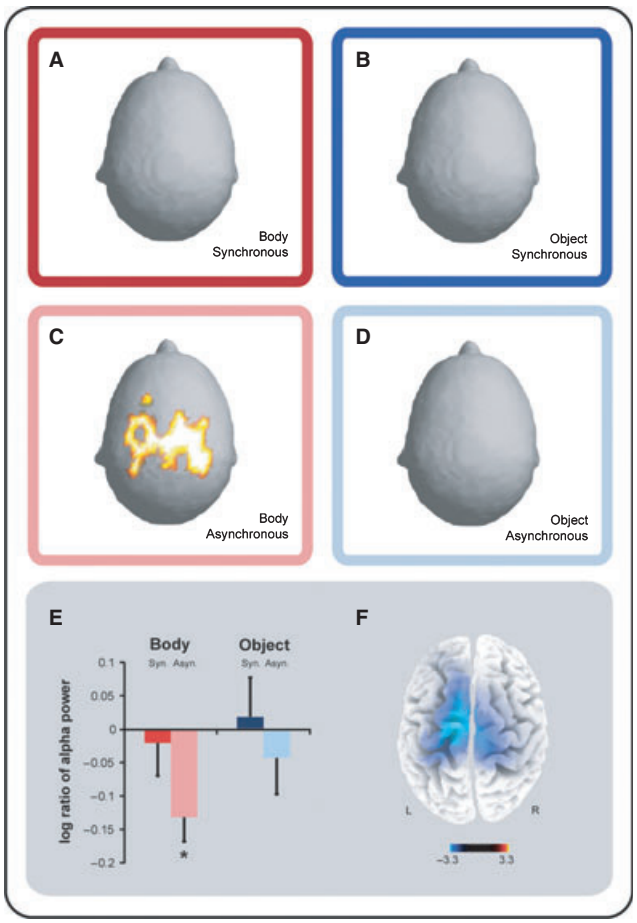

FIG. 3. Alpha power modulation over sensorimotor areas. (A–D) Statistical maps of significant alpha band (8–13 Hz) modulation for all four experimental conditions compared with the visual control condition (compare with Fig. 1E). Analysis was carried out on all 256 scalp electrodes, and statistical results are plotted as projected on the scalp. Note that due to the nature of the cluster test the colour indicates significance in a binary fashion: yellow for significance and grey for non-significance. The top view is shown (nose on top and back of the head at the bottom for each plot). Analysis of the body asynchronous condition (B) shows a large significant cluster of 23 electrodes ($P = 0.046$), where alpha band power was suppressed as compared with the visual control condition. The highlighted scalp areas showed significant alpha band suppression as defined by a permutation test (see Materials and methods). No significant suppression or enhancement was observed in the body synchronous condition (A) and either object condition (B and D). (E) Changes in alpha power (mean ± SEM) for the sensorimotor cluster (23 electrodes, see B) are shown for all four experimental conditions as compared with the visual control condition. *Indicates the significant alpha power suppression for the asynchronous body condition as compared with baseline ($P < 0.05$). (F) Inverse solution of the contrast body asynchronous vs visual control showing alpha band suppression in medial sensorimotor and premotor cortices (centred on the precentral gyrus and posterior superior frontal gyrus; $F = 3.29$).

different from the activation in the visual-only condition (Fig. 3). The data of these direct comparisons can be found in the Supporting Information (Fig. S4).

Gamma band power

We used two-sided *t*-tests (with the log of the gamma power value for each electrode) to compare each condition with the visual control condition. None of the clusters reached a significant cluster size (the most significant cluster had three electrodes; $P = 0.42$). For more detailed data see the Supporting Information (Fig. S3). Analysis for the broad gamma band (30–99 Hz) also did not reveal any significant cluster (the most significant cluster had four electrodes; $P = 0.47$). The results for the direct comparisons between synchronous vs asynchronous conditions (performed separately for body and control object conditions) revealed no significant difference and can be found in the Supporting Information (Fig. S5).

Correlation between drift and band power

Alpha band power

We next searched for areas in which changes in EEG activity were related to changes of self-location due to experimental manipulation by analysing correlations between the size of the drift and the change in EEG alpha band power (and gamma power, see next paragraph). To obtain the strongest contrast in illusory self-location we looked at the difference between the synchronous and asynchronous conditions and calculated the correlation for this difference in both drift and alpha power for each electrode separately for body and the object (see Materials and methods). The results showed a large cluster of electrodes in a single scalp region over the medial prefrontal cortex (mPFC; and premotor cortex; 31 electrodes; $P = 0.048$; Fig. 4, upper panel), revealing positive correlations between alpha power and drift, as measured by the difference between the synchronous and asynchronous conditions (max. $R = 0.90$, mean $R = 0.68$). A smaller region of electrodes was found over the parieto-occipital cortex, but the cluster size was not significant (six electrodes; $P = 0.19$). The same analysis was done for the control object condition and no significantly correlated clusters were found. The positive correlation in the body condition, together with our observation that the drift in the synchronous body condition is mostly positive (as compared with the asynchronous condition), shows that participants with larger changes in self-location between the synchronous and asynchronous body condition show larger alpha band power differences in electrodes over the mPFC. sLORETA located this change in EEG alpha band power to medio-dorsal PFC, centred in the left superior frontal gyrus (MNI: $X = 20$, $Y = 40$, $Z = 50$; Fig. 5).

Gamma band power

We found three clusters of electrodes showing a correlation between the gamma band power and illusory self-location (analysed in the same way as the alpha power; Fig. 4, lower panel). The largest cluster (showing a negative correlation) was found over the right temporo-parietal junction (TPJ) region (12 electrodes; $P = 0.18$), an area that we predicted to be involved based on previous clinical data (e.g. Blanke *et al.*, 2002); however, it did not reach significance ($P = 0.05$ corresponded to a cluster size of 22 electrodes). Two smaller clusters over midline regions (parieto-occipital: nine electrodes, $P = 0.25$; central: 7 electrodes, $P = 0.32$) revealed positive correlations. Analysis in the broad gamma band (30–99 Hz) did not reveal a significant cluster (the most significant cluster had four electrodes, $P = 0.47$).

Discussion

By merging VR with cognitive psychology and high-resolution EEG, we used multisensory conflicts to induce changes in self-location. The analysis of alpha band, but not gamma band, highlighted two areas that we found to be associated with these changes. As predicted, bilateral sensorimotor and premotor cortices were differentially activated in synchronous and asynchronous body conditions. We also found that the strength of the mPFC activity correlated with the strength of illusory self-location. Along with providing insights into the brain mechanisms of human bodily self-consciousness, our

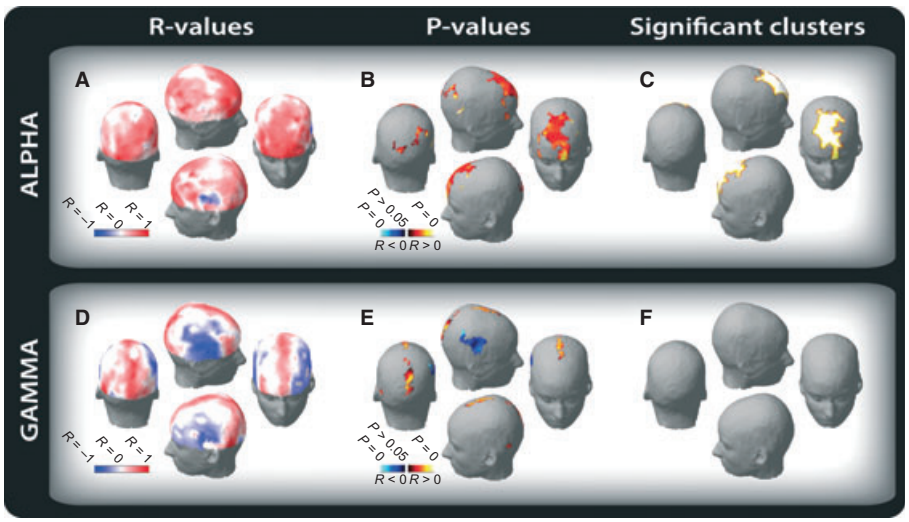

FIG. 4. Correlation between band power and self-localization. This figure shows the correlation between the drift in self-localization and band power for the synchronous (relative to the asynchronous) body condition. The top row (A–C) shows the correlation for the alpha band (8–13 Hz), while the bottom row (D–F) shows the correlation for the gamma band (30–49 Hz) Left (A and D): correlation coefficients (*R*-values, red indicating a positive, blue a negative correlation); middle (B and E): statistical maps (coloured areas indicate electrodes with significant correlations $P < 0.05$); right (C and F): significant clusters after correction for multiple testing. Note that the colour in (C) and (F) indicates significance in a binary fashion: yellow for significance and grey for non-significance. For the alpha band we see a large significant cluster (C) of positive correlation over medial frontal areas (31 electrodes, $P = 0.048$, max $R = 0.90$, mean $R = 0.68$). For the gamma band we see a cluster of negative correlation over the TPJ and a cluster of positive correlation over the precuneus (E), but these clusters did not reach the significant cluster size (F).

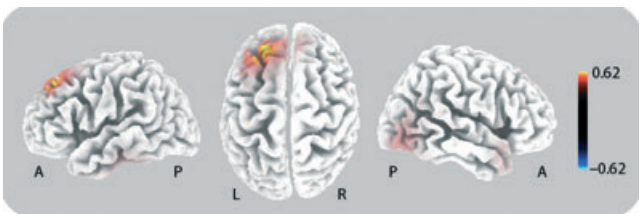

FIG. 5. Inverse solution of correlation between band power and self-localization. This figure shows the inverse solution of the correlation between the drift in self-localization and alpha band power. It shows a positive correlation in the medio-dorsal PFC (centred on the superior frontal gyrus; $R = 0.62$).

findings highlight the potential of high-resolution EEG to be used with VR set-ups, enabling ecologically valid presentation of life-sized bodily stimuli (see also Sanchez-Vives & Slater, 2005).

Bodily self-consciousness

VR technology permitted fine-grained experimental control of visual and tactile stimulation. It also enabled us, unlike previous studies (Ehrsson, 2007; Lenggenhager *et al.*, 2007), to independently control the synchrony of the stroking and of own body movements. The participants' own small body movements were always displayed synchronously on the virtual body (or the control object), while the stroking was shown independently either synchronously or not. The present behavioural data confirm our previous findings (Lenggenhager *et al.*, 2007), showing that participants localized themselves closer to the virtual body in the synchronous than in the asynchronous condition. This effect was no longer significant in the control object condition. Using this new experimental set-up we were able to induce illusory self-location. This brings neurological observations (Brugger *et al.*, 1997; Blanke *et al.*, 2004) on patients with disturbed bodily self-consciousness where such multisensory conflict may occur due to focal brain damage under scientific scrutiny.

Alpha band modulations in sensorimotor and premotor cortices

One of the main findings of the present study is that alpha band power (8–13 Hz) in a large bilateral area at central and frontal scalp electrodes was differentially suppressed in the synchronous and asynchronous conditions. Source localization cited these power changes to bilateral medial sensorimotor and premotor cortices. The suppression was body-specific in the sense that alpha band power was only modulated by synchrony when the stroking was shown on the virtual body and not on the control object – these alpha band oscillations differed most strongly in those conditions inducing the strongest changes in self-location.

The alpha band oscillation over central areas (mu rhythm) has been linked to sensorimotor processing (for a review, see Pineda, 2005). Mu rhythm suppression (caused by neuronal desynchronization) is thought to reflect increased cortical activation in sensorimotor and/or premotor cortices (Oakes *et al.*, 2004). Action-related tasks such as action execution and observation (Gastaut, 1952), motor imagery (Pfurtscheller & Neuper, 1997), and biological motion perception (Ulloa & Pineda, 2007) have been shown to suppress the mu rhythm in the sensorimotor cortex. Similarly, in the somatosensory system, touch (Pfurtscheller, 1981) as well as the observation of touch of another person (Cheyne *et al.*, 2003) result in mu suppression over sensorimotor areas. The present EEG data also reveal an activation of sensorimotor and premotor cortices. The medial location in the sensorimotor cortex is compatible with an activation of sensorimotor cortex encoding the trunk region (e.g. Penfield & Jaspers, 1954; Kaas *et al.*, 1979; Lesser *et al.*, 1987; Itomi *et al.*, 2000). We found that the scalp cluster and the brain activation extend bilaterally (left-hemispheric predominance in the inverse solution), which is probably related to the fact that the stroking was applied to both sides of the participants' back and that trunk receptive fields are represented bilaterally in the primary somatosensory cortex and higher-tier parietal areas (Eickhoff *et al.*, 2006). Activations (Fig. 3) extend to the premotor cortex. Previous work suggested that the mu rhythm at fronto-central scalp electrodes may reflect mirror neuron-related

activity in the premotor cortex (Pineda, 2005), and has also been reported in the medial premotor cortex in humans (Mukamel *et al.*, 2007). Premotor neurons have previously been shown to encode visual and tactile stimuli in a body-centred reference frame (e.g. Graziano *et al.*, 2000; Graziano & Botvinick, 2002), and are involved in the rubber hand illusion (Ehrsson *et al.*, 2004). Although tonic activation of the alpha band has been linked to visual attention (e.g. Dockree *et al.*, 2007), such mechanisms are not likely to account for the reported differences in sensorimotor and premotor cortices as the present effects were body-specific.

We note that our EEG data suggest a greater activation of sensorimotor and premotor cortices during asynchronous visual–tactile stimulation, extending PET data during a related illusion (Tsakiris *et al.*, 2007). These authors found increased blood flow in contralateral sensorimotor cortex (pre- and postcentral gyri) during asynchronous hand visuo-tactile stimulation. The difference in the lateralization of brain activation (contralateral for the hand, Tsakiris *et al.*, 2007; bilateral and more medial for trunk, present study) during asynchronous visuo-tactile stimulation suggests that changes in bodily self-consciousness concerning hand or trunk activate partly similar but also distinct brain regions (Blanke & Metzinger, 2009). Such comparisons should, however, be regarded with caution, as neither study performed a direct comparison between hand and back-stroking, and because the behavioural methods and the brain imaging methods differed. Stronger activations in the asynchronous body condition could be related to mechanisms of greater multisensory bodily conflict (Fink *et al.*, 1999; Tsakiris *et al.*, 2007). Whereas in the asynchronous and synchronous body conditions participants were exposed to spatial incongruency between the seen (virtual body on the screen) and the felt body (participant's body), there was a second conflict only in the asynchronous body condition – spatial incongruency concerning the relative location of touch on the back. Stronger activations in the asynchronous body condition could thus also be related to mechanisms for interpreting somatosensory information and for the 'simulation' of observed tactile events (Keysers *et al.*, 2004). This is also suggested by directly comparing brain activations between the body synchronous vs body asynchronous condition. This comparison revealed an activation pattern that was highly similar to the body asynchronous vs visual-only comparison (yet with opposite sign; Fig. 3 and Supporting Information Fig. S4). This suggests that the observed difference in mu power in the sensorimotor cortex between the synchronous and asynchronous body conditions is mainly due to the visuo-tactile conflict (relative location of touch on the back as described above), also because the brain activations during synchronous and the visual-only conditions that lack the visuo-tactile conflict are similar, but show differences in self-location. More work is necessary to further distinguish differential brain activations related to different visuo-tactile conflicts and changes in bodily self-consciousness.

Alpha band modulations in the medio-dorsal PFC and self-location

Another main finding was the effect of self-location in the medio-dorsal PFC. The strength of alpha power in the mPFC (with a peak in the superior frontal gyrus) revealed a positive correlation with the strength of illusory self-location. This positive correlation, only found in the body condition, suggests that participants who showed greater modulation in self-location also show greater modulation of the alpha band power in the mPFC. This finding links self-location to the mPFC, an area thought to be a key region in self-related processing (Northoff *et al.*, 2006). The PFC, and notably the mPFC, is associated with a large variety of self-related cognitions, such as own name recognition (Perrin *et al.*, 2005), memory for self-traits (Macrae *et al.*, 2004), linguistic self-reference (Esslen *et al.*, 2008), perspective taking (Vogeley & Fink, 2003) and self-other discrimination (Heatherton *et al.*, 2006). This association to conceptual, mnestic, affective, perspectival, as well as to perceptual aspects of the self, is compatible with deficits in self-related processing in patients with mPFC abnormalities (Sturm *et al.*, 2006; Broyd *et al.*, 2009). Furthermore, two recent observations in neurological patients with disturbed frontal processing were shown to suffer from specific alterations of global bodily self-consciousness (self-location and self-identification; Heydrich *et al.*, 2010; Lopez *et al.*, 2010). Due to the relatively low spatial resolution of EEG data in medial regions (even for multichannel EEG), we do not know whether the observed mPFC activation is related to all or only certain subregions of the mPFC, such as anterior cingulate, supplementary motor area (SMA) or superior frontal gyrus. Further neuroimaging work is necessary to reveal the detailed anatomical and electrophysiological distinctions in the mPFC with respect to bodily self-consciousness.

Based on the present correlation analysis, we suggest that participants with a stronger bias in self-location show increased alpha power, presumably reflecting decreased mPFC activation (Laufs *et al.*, 2003). Accordingly, we argue that the amount of mPFC activation may reflect the robustness of self-location – the conscious experience of being localized at the position of one's physical body. As such, strong mPFC cortex activation reflects a robust spatial self-representation (normal self-location), whereas weak mPFC activation is associated with a weaker and abnormal spatial self-representation (illusory self-location). This correlation was only found when participants were exposed to a virtual body, and was not found in control conditions, suggesting that this result is not caused by attentional biases. Our data suggest that the mPFC activation, associated mostly with high-order aspects of self-processing (Northoff *et al.*, 2006), also reflects low-level multisensory conflict resulting in changes in bodily self.

Supporting Information

Additional supporting information may be found in the online version of this article:

Fig. S1. Power-spectra for the sensorimotor cluster.
Fig. S2. Alpha band modulations as compared to the visual baseline.
Fig. S3. Gamma band modulations as compared to the visual baseline.
Fig. S4. Alpha band modulations during synchronous stroking as compared to asynchronous stroking.
Fig. S5. Gamma band modulations during synchronous stroking as compared to asynchronous stroking.

Please note: As a service to our authors and readers, this journal provides supporting information supplied by the authors. Such materials are peer-reviewed and may be re-organized for online delivery, but are not copy-edited or typeset by Wiley-Blackwell. Technical support issues arising from supporting information (other than missing files) should be addressed to the authors.

Acknowledgements

The authors are grateful for support by the Swiss National Science Foundation and the Fondation de Famille Sandoz. Olaf Blanke is supported by the Swiss National Science Foundation (grant number SINERGIA CRSII1-125135/1). We thank Lars Schwabe for his essential programming contribution to the Motionbuilder setup. We also thank Jane Aspell and Nathan Evans for proofreading.

Abbreviations

EEG, electroencephalogram; FFT, Fast Fourier Transform; LED, light-emitting diode; mPFC, medial prefrontal cortex; PET, positron emission tomography; PFC, prefrontal cortex; VR, virtual reality.

References

Aspell, J.E., Lenggenhager, B. & Blanke, O. (2009) Keeping in touch with one's self: multisensory mechanisms of self-consciousness. *PLoS ONE*, **4**, e6488.

Berlucchi, G. & Aglioti, S. (1997) The body in the brain: neural bases of corporeal awareness. *Trends Neurosci.*, **20**, 560–564.

Blackman, R.B. & Tukey, J.W. (1959). *The Measurement of Power Spectra from the Point of View of Communications Engineering*. Dover, New York.

Blanke, O. & Metzinger, T. (2009) Full-body illusions and minimal phenomenal selfhood. *Trends Cogn. Sci.*, **13**, 7–13.

Blanke, O., Ortigue, S., Landis, T. & Seeck, M. (2002) Stimulating illusory own-body perceptions. *Nature*, **419**, 269–270.

Blanke, O., Landis, T., Spinelli, L. & Seeck, M. (2004) Out-of-body experience and autoscopy of neurological origin. *Brain*, **127**, 243–258.

Broyd, S.J., Demanuele, C., Debener, S., Helps, S.K., James, C.J. & Sonuga-Barke, E.J. (2009) Default-mode brain dysfunction in mental disorders: a systematic review. *Neurosci. Biobehav. Rev.*, **33**, 279–296.

Brugger, P., Regard, M. & Landis, T. (1997) Illusory reduplication of one's own body: phenomenology. classification of autoscopic phenomena. *Cogn. Neuropsychiatry*, **2**, 19–38.

Cheyne, D., Gaetz, W., Garnero, L., Lachaux, J.P., Ducorps, A., Schwartz, D. & Varela, F.J. (2003) Neuromagnetic imaging of cortical oscillations accompanying tactile stimulation. *Brain Res. Cogn. Brain Res.*, **17**, 599–611.

De Ridder, D., Van Laere, K., Dupont, P., Menovsky, T. & Van de Heyning, P. (2007) Visualizing out-of-body experience in the brain. *N. Engl. J. Med.*, **357**, 1829–1833.

Dockree, P.M., Kelly, S.P., Foxe, J.J., Reilly, R.B. & Robertson, I.H. (2007) Optimal sustained attention is linked to the spectral content of background EEG activity: greater ongoing tonic alpha (approximately 10 Hz) power supports successful phasic goal activation. *Eur. J. Neurosci.*, **25**, 900–907.

Ehrsson, H.H. (2007) The experimental induction of out-of-body experiences. *Science*, **317**, 1048.

Ehrsson, H.H., Spence, C. & Passingham, R.E. (2004) That's my hand! Activity in premotor cortex reflects feeling of ownership of a limb. *Science*, **305**, 875–877.

Eickhoff, S.B., Weiss, P.H., Amunts, K., Fink, G.R. & Zilles, K. (2006) Identifying human parieto-insular vestibular cortex using fMRI and cytoarchitectonic mapping. *Hum. Brain Mapp.*, **27**, 611–621.

Esslen, M., Metzler, S., Pascual-Marqui, R. & Jancke, L. (2008) Pre-reflective and reflective self-reference: a spatiotemporal EEG analysis. *Neuroimage*, **42**, 437–449.

Fink, G.R., Marshall, J.C., Halligan, P.W., Frith, C.D., Driver, J., Frackowiak, R.S. & Dolan, R.J. (1999) The neural consequences of conflict between intention and the senses. *Brain*, **122**, 497–512.

Fuchs, M., Kastner, J., Wagner, M., Hawes, S. & Ebersole, J.S. (2002) A standardized boundary element method volume conductor model. *Clin. Neurophysiol.*, **113**, 702–712.

Gallagher, S. (2005) *How the Body Shapes the Mind*. Oxford University Press, Oxford.

Gastaut, H. (1952) Electrocorticographic study of the reactivity of rolandic rhythm. *Rev. Neurol. (Paris)*, **87**, 176–182.

Graziano, M.S.A. & Botvinick, M. (2002) How the brain represents the body: insights from neurophysiology and psychology. In Prinz, W. & Hommel, B. (eds), *Common Mechanisms in Perception and Action: Attention and Performance XIX*. Oxford University Press, Oxford, pp. 136–157.

Graziano, M.S.A., Cooke, D.F. & Taylor, C.S. (2000) Coding the location of the arm by sight. *Science*, **290**, 1782–1786.

Heatherton, T.F., Wyland, C.L., Macrae, C.N., Demos, K.E., Denny, B.T. & Kelley, W.M. (2006) Medial prefrontal activity differentiates self from close others. *Soc. Cogn. Affect. Neurosci.*, **1**, 18–25.

Heydrich, L., Dieguez, S., Grunwald, T., Seeck, M. & Blanke, O. (2010) Illusory own body perceptions: case reports and relevance for bodily self-consciousness. *Conscious. Cogn.*, **19**, 702–710.

Heydrich, L., Lopez, C., Seek, M. & Blanke, O. (2011). Partial and full own body illusions of eplipeptic origin in a child with right temporo-parietal epilepsy. *Epilepsy Behav.*, doi:10.1016/j.physletb.2003.10.071 [Epub ahead of print].

Itomi, K., Kakigi, R., Maeda, K. & Hoshiyama, M. (2000) Dermatome versus homunculus; detailed topography of the primary somatosensory cortex following trunk stimulation. *Clin. Neurophysiol.*, **111**, 405–412.

Kaas, J.H., Nelson, R.J., Sur, M., Lin, C.S. & Merzenich, M.M. (1979) Multiple representations of the body within the primary somatosensory cortex of primates. *Science*, **204**, 521–523.

Kanayama, N., Sato, A. & Ohira, H. (2007) Crossmodal effect with rubber hand illusion and gamma-band activity. *Psychophysiology*, **44**, 392–402.

Kanayama, N., Sato, A. & Ohira, H. (2009) The role of gamma band oscillations and synchrony on rubber hand illusion and crossmodal integration. *Brain Cogn.*, **69**, 19–29.

Keysers, C., Wicker, B., Gazzola, V., Anton, J.L., Fogassi, L. & Gallese, V. (2004) A touching sight: SII/PV activation during the observation and experience of touch. *Neuron*, **42**, 335–346.

Lackner, J.R. & DiZio, P.A. (2000) Aspects of body self-calibration. *Trends Cogn. Sci.*, **4**, 279–288.

Laufs, H., Kleinschmidt, A., Beyerle, A., Eger, E., Salek-Haddadi, A., Preibisch, C. & Krakow, K. (2003) EEG-correlated fMRI of human alpha activity. *Neuroimage*, **19**, 1463–1476.

Lenggenhager, B., Tadi, T., Metzinger, T. & Blanke, O. (2007) Video ergo sum: manipulating bodily self-consciousness. *Science*, **317**, 1096–1099.

Lenggenhager, B., Mouthon, M. & Blanke, O. (2009) Spatial aspects of bodily self-consciousness. *Conscious. Cogn.*, **18**, 110–117.

Lesser, R.P., Luders, H., Klem, G., Dinner, D.S., Morris, H.H., Hahn, J.F. & Wyllie, E. (1987) Extraoperative cortical functional localization in patients with epilepsy. *J. Clin. Neurophysiol.*, **4**, 27–53.

Lopez, C., Heydrich, L., Seeck, M. & Blanke, O. (2010) Abnormal self-location and vestibular vertigo in a patient with right frontal lobe epilepsy. *Epilepsy Behav.*, **17**, 289–292.

Macrae, C.N., Moran, J.M., Heatherton, T.F., Banfield, J.F. & Kelley, W.M. (2004) Medial prefrontal activity predicts memory for self. *Cereb. Cortex*, **14**, 647–654.

Maris, E. & Oostenveld, R. (2007) Nonparametric statistical testing of EEG- and MEG-data. *J. Neurosci. Methods*, **164**, 177–190.

Metzinger, T. (2007) Empirical perspectives from the self-model theory of subjectivity: a brief summary with examples. *Prog. Brain Res.*, **168**, 215–278.

Mukamel, R., Ekstrom, A., Kaplan, J., Iacoboni, M. & Fried, I. (2007) Mirror properties of single cells in human medial frontal cortex. *Soc. Neurosci.*. Abstract 127, Atlanta.

Nichols, T.E. & Holmes, A.P. (2002) Nonparametric permutation tests for functional neuroimaging: a primer with examples. *Hum. Brain Mapp.*, **15**, 1–25.

Northoff, G., Heinzel, A., de Greck, M., Bermpohl, F., Dobrowolny, H. & Panksepp, J. (2006) Self-referential processing in our brain – a meta-analysis of imaging studies on the self. *Neuroimage*, **31**, 440–457.

Oakes, T.R., Pizzagalli, D.A., Hendrick, A.M., Horras, K.A., Larson, C.L., Abercrombie, H.C., Schaefer, S.M., Koger, J.V. & Davidson, R.J. (2004) Functional coupling of simultaneous electrical and metabolic activity in the human brain. *Hum. Brain Mapp.*, **21**, 257–270.

Oberman, L.M., Hubbard, E.M., McCleery, J.P., Altschuler, E.L., Ramachandran, V.S. & Pineda, J.A. (2005) EEG evidence for mirror neuron dysfunction in autism spectrum disorders. *Brain Res. Cogn. Brain Res.*, **24**, 190–198.

Pascual-Marqui, R.D. (2002) Standardized low-resolution brain electromagnetic tomography (sLORETA): technical details. *Methods Find. Exp. Clin. Pharmacol.*, **24**, 5–12.

Penfield, W. & Jaspers, H. (1954) *Epilepsy and the Functional Anatomy of the Human Brain*. Little Brown, Boston.

Perrin, F., Maquet, P., Peigneux, P., Ruby, P., Degueldre, C., Balteau, E., Del Fiore, G., Moonen, G., Luxen, A. & Laureys, S. (2005) Neural mechanisms involved in the detection of our first name: a combined ERPs and PET study. *Neuropsychologia*, **43**, 12–19.

Petkova, V.I. & Ehrsson, H.H. (2008) If I were you: perceptual illusion of body swapping. *PLoS ONE*, **3**, e3832.

Pfurtscheller, G. (1981) Central beta rhythm during sensorimotor activities in man. *Electroencephalogr. Clin. Neurophysiol.*, **51**, 253–264.

Pfurtscheller, G. & Neuper, C. (1997) Motor imagery activates primary sensorimotor area in humans. *Neurosci. Lett.*, **239**, 65–68.

Pineda, J.A. (2005) The functional significance of mu rhythms: translating "seeing" and "hearing" into "doing". *Brain Res. Brain Res. Rev.*, **50**, 57–68.

Sanchez-Vives, M.V. & Slater, M. (2005) From presence to consciousness through virtual reality. *Nat. Rev. Neurosci.*, **6**, 332–339.

Senkowski, D., Talsma, D., Grigutsch, M., Herrmann, C.S. & Woldorff, M.G. (2007) Good times for multisensory integration: effects of the precision of temporal synchrony as revealed by gamma-band oscillations. *Neuropsychologia*, **45**, 561–571.

Sturm, V.E., Rosen, H.J., Allison, S., Miller, B.L. & Levenson, R.W. (2006) Self-conscious emotion deficits in frontotemporal lobar degeneration. *Brain*, **129**, 2508–2516.

Tadi, T., Overney, L.S. & Blanke, O. (2009) Three sequential brain activations encode mental transformations of upright and inverted human bodies: a high resolution evoked potential study. *Neuroscience*, **159**, 1316–1325.

Tsakiris, M., Hesse, M.D., Boy, C., Haggard, P. & Fink, G.R. (2007) Neural signatures of body ownership: a sensory network for bodily self-consciousness. *Cereb. Cortex*, **17**, 2235–2244.

Ulloa, E.R. & Pineda, J.A. (2007) Recognition of point-light biological motion: mu rhythms and mirror neuron activity. *Behav. Brain Res.*, **183**, 188–194.

Vogeley, K. & Fink, G.R. (2003) Neural correlates of the first-person-perspective. *Trends Cogn. Sci.*, **7**, 38–42.